JSML
Journal of Science and Mathematics Letters
Universiti Pendidikan Sultan Idris
ISSN 2462-2052 • eISSN 2600-8718

Research Article

Biogenic $Co_3CuCr_2O_8$ Nanocomposites Prepared Using *Olea europaea* Leaf Extract as a Nanoantibacterial Platform for Dental Caries Management

Riyam Lateef Khalaf*, Mina Mohammed Kadhim, Abdalwahab Malath Alhadithi, Ola Abdul Kareem Nori

Ibn Sina University of Medical and Pharmaceutical Sciences, Al-Qadisiyah Road, Baghdad 10011, Iraq
* Corresponding author: riyam.lateef@ibnsina.edu.iq

ARTICLE HISTORY

Received
19 March 2026
Revised
18 June 2026
Accepted
10 July 2026
Published
23 July 2026

KEYWORDS

Olea europaea
nanotechnology
cobalt-copper-chromium
nanocomposite
antibacterial
dental infections

ABSTRACT

The present work investigates the rapid synthesis of a Cobalt-Copper-Chromium nanocomposite by a biological method using *Olea europaea* leaf extract and Cobalt-Copper-Chromium salt as precursors. Cobalt-Copper-Chromium nanocomposite was successfully synthesized from *O. europaea* leaves extracted using a Green synthesis technique. UV-Visible Spectroscopy, Field Emission Scanning Electron Microscopy (FESEM), X-ray Diffraction (XRD), Fourier Transform Infrared (FTIR), and Transmission Electron Microscopy (TEM) were used to characterize the Cobalt-Copper-Chromium nanocomposites in detail. These measurements show that these Cobalt-Copper-Chromium nanocomposites had a spherical shape with a diameter of 45.7 to 51.6 nm and were stable for at least two months. Finally, the antibacterial activity of the $Co_3CuCr_2O_8$ nanocomposite was evaluated against oral pathogenic bacteria associated with dental caries, including *Streptococcus mutans*, *Streptococcus mitis*, and *Staphylococcus lentus*. The results demonstrated a strong concentration-dependent inhibitory effect, with oral *streptococci* exhibiting higher sensitivity than *S. lentus*. To assess biosafety, cytotoxicity was evaluated on normal human dermal fibroblast (HDF) cells using the MTT assay after 48 h of exposure. The nanocomposite showed concentration-dependent cytotoxicity, with high cell viability (>80%) observed at higher dilutions (≥1:80), indicating good cytocompatibility under controlled conditions. Overall, the results demonstrate that the green-synthesized $Co_3CuCr_2O_8$ nanocomposite combines effective antibacterial activity with acceptable biocompatibility, supporting its potential application in dental and biomedical fields.

https://doi.org/10.37134/jsml.vol14.3.6.2026

1. INTRODUCTION

Nanotechnology is a fast-expanding scientific topic that has garnered a lot of attention in recent years. In contrast to the chemical and physical methods currently used for nanosynthesis, green nanotechnology is a multidisciplinary field that has emerged as a rapidly developing research area. It serves as an important technique that emphasizes making the procedure clean, non-hazardous, and especially environmentally friendly (Saratale et al., 2018). Biomolecules reduce metal ions, leading to nucleation and growth of nanoparticles, while other compounds stabilize them. *O. europaea* leaves are rich in bioactive compounds such as polyphenols, flavonoids, and oleuropein. These compounds act as reducing and capping agents (Shafey, 2020; Khudiar et al., 2022)

Metal oxides have shown promising advancements in various fields, particularly in biomedical applications (Jeon et al., 2022). The nanocomposite consists of a multiphase solid material where one of the phases has one, two, or three dimensions of less than 100 nm or structures having nanoscale repeat distances between the different phases that make up the material. The concept behind nanocomposites is to develop and produce novel materials with previously unheard-of flexibility and improved physical qualities using building blocks with diameters in the nanometer range. Depending on the composition of nanomaterial, size, and dosage of each material, nanocomposites have potential antibacterial properties, making them useful for medicinal applications (Mohammed-Salih et al., 2025).

Nanocomposite materials have been found to be a promising multifunctional platform for biomedical applications due to their unique physicochemical properties, biocompatibility, and enhanced therapeutic potential. The versatility of this has enabled them to create new and innovative strategies for the treatment of microbial infections, drug delivery, tissue regeneration, and even diagnostic technologies (Mohammed-Salih et al., 2024). A variety of nanocomposites have demonstrated distinct physicochemical characteristics, biocompatibility, and biodegradability by reinforcing synthetic and natural polymers with nanoparticles (Mamidi et al., 2025). The development of advanced hybrid nanocomposites incorporating metal oxides with sustainable plant extracts such as *O. europaea* leaf extract has resulted in materials with controlled particle sizes and enhanced properties (Umai et al., 2021; Joy et al., 2022; Al-Deen et al., 2026).

The benefits of local medication administration in dental caries include targeted treatment and fewer side effects. In recent years, the use of nanotechnology in this context has become more and more popular. Here is a quick summary of the latest advancements in the local treatment of dental caries utilizing nanoparticles, based on a review of the literature. Because of their tiny size and improved penetration, nanoparticles can be used as delivery methods to entrap chemicals or medications. Additionally, they can benefit from using biomimetic techniques to treat patients more successfully (Ahmadian et al., 2018). Hasanin et al. (2024) demonstrated their effectiveness against bacteria such as *Salmonella typhimurium* and *Staphylococcus aureus*, as well as fungi like *Candida albicans*. Also, they show potential in cancer treatment, displaying cytotoxic effects against cancerous cell line. The human oral cavity is a complex ecosystem harboring a diverse microbiota, with over 700 species of bacteria identified, alongside fungi, viruses, and protozoa (Selvanayaki et al., 2022; Joy et al., 2022). While many of these microorganisms are commensals (e.g., *S. mitis*) that coexist beneficially, *S. mutans* is strongly associated with dental caries.

Coexisting in a beneficial manner with their host, contributing to oral homeostasis, an imbalance can lead to significant dental problems (Yadav & Prakash, 2017). Dental caries is the most common oral disorder in the world. The oral microbiota is closely related to the development of dental caries (Zhang et al., 2022). Of particular importance, certain bacteria, such as *S. mutans*, are known to be involved in the pathogenesis of dental caries (tooth decay) by converting dietary sugars into acids that demineralize tooth enamel (Jaffar et al., 2023). Moreover, oral bacteria can also degrade the durability of dental restorations, leading to secondary caries (new decay formation) in the margins or under the existing restoration, by colonizing the micro gaps and generating acids that attack the surrounding tooth structure (Yazdanian et al., 2022; Esfanddarani & Panigrahi, 2024). Understanding the types of oral bacteria and their impact on both natural teeth and dental materials is essential for developing effective strategies for maintaining oral health. Microbial diversity declines as caries progresses, while the strength of microbial interactions increases (Shao et al., 2023). The incorporation of Cobalt-Copper-Chromium nanocomposite into dental restorative materials may be a promising approach to inhibit biofilm formation and prolong the life of restorations. Prior studies have shown that Cu and Co nanoparticles can be embedded into dental composites or coatings to provide both mechanical strength and antimicrobial functionality (Tariq et al., 2026).

Moreover, chromium nanoparticles, though less studied in dentistry, have demonstrated anti-adhesive and bacteriostatic effects in biomedical applications (Mendes et al., 2022), suggesting their potential use in oral environments. Oral pathogenic bacteria are an important factor in the pathogenesis of dental diseases such as dental caries and periodontal infections. Because of its ability to form a strong biofilm and produce acid, *S. mutans* is known as the main etiological agent of dental caries, which leads to the demineralization of enamel (Lemos et al., 2019). *S. mitis* is an early colonizer of the oral cavity and is involved in the development of dental plaque and as a substrate for the adhesion of other pathogenic microorganisms (Engen et al., 2017). *S. lentus* is not a common oral pathogen but is an opportunistic pathogen that can cause infection under compromised conditions and has been reported to have antimicrobial resistance, thus being a good model for assessment of the antibacterial activity of newly synthesized nanomaterials. Hence, these bacterial species were chosen to evaluate the wide range of antibacterial activities of the synthesized $Co_3CuCr_2O_8$ nanocomposite.

The present study was designed to synthesize $Co_3CuCr_2O_8$ nanocomposites by the green synthesis method, determine their physicochemical properties, assess their antibacterial activity against oral pathogens, and cytotoxicity towards human dermal fibroblast cells.

2. METHODOLOGY

2.1. Material

All chemicals and biological materials were used are Urea (NH_2CONH_2) (Sigma-Aldrich/USA), cobalt nitrate $Co(NO_3)_2$ (Merck/ Germany), copper chloride $CuCl_2$ (Merck/ Germany), chroumium sulphate $Cr_2(SO_4)_3$ (Merck/ Germany), Sodium hydroxide NaOH (Fulka/ Swiss), Brain heart infusion (biotrend/ Germany), macconkey agar (biotrend/ Germany), HDF cell lines (ATCC), MCF7 cell lines (ATCC), RPMI1640 (Biowest, France), DMEM high glucose (Biowest, France), Fetal Bovine Serum (FBS) (Biowest, France), Penicillin/Streptomycin (Biowest, France), DMSO (Merck, Germany), MTT reagent (Merck, Germany), ELISA Reader (BioRad, USA), Pipettes and sterile syringes (SPL, China),96-well sterile tissue culture plates (SPL, China). Nanocomposite synthesis: Individually, the metal sources (cobalt, copper and chromium) were used in a stoichiometric ratio (1:1:1) to prepare ternary oxides of the nanocomposite. Accordingly, 0.01 M of each $Co(NO_3)_2$, $CuCl_2$, and $Cr_2(SO_4)_3$ were mixed at 25°C and pH 4.

2.2. Synthesize of Cobalt-Copper-Chromium Nanocomposite

To synthesize the Cobalt-Copper-Chromium nanocomposite, 2 mL of *O. europaea* leaf extract were added dropwise to 5 mL of 0.01 M of the stock solution Cobalt-Copper-Chromium; the volume was filled to 50 mL with distilled water, and the sample was stirred and heated for 15 min at 70°C. Then centrifuged for 15 min at 4000 RPM to precipitate the nanocomposite and washed several times to remove the contamination. The sample was then dried, yielding the Cobalt-Copper-Chromium nanocomposite for characterization. Fourier transform infrared (FTIR) spectra were obtained at room temperature on a Shimadzu FTIR 84005 spectrometer for the plant extract containing Cobalt-Copper-Chromium nanocomposite (0.01 g) dried at 60ºC for 4 h using KBr (Khalaf et al., 2021a), then calcination at 300ºC for 3 h to synthesize nanooxide. An X-ray Diffraction (XRD) pattern was produced using a Shimadzu XRD-6000 diffractometer with Cu Kα (λ=1.54056 A°) to validate the biosynthesis of nanocomposite (Khalaf & Ahmed, 2019). The morphology and surface morphology of the nanocomposite were examined using a FESEM S-4160 (Khalaf et al., 2021b). Transmission electron microscopy (TEM) was performed to investigate the particle morphology and size distribution of the synthesized nanocomposite, and particle sizes were determined using ImageJ software.

2.3. Application of the Nanocomposite

2.3.1. Sample Collection

A total of 20 patients with similar oral hygiene levels were selected for this experiment. Ten patients were selected to receive amalgam fillings, while another ten patients were selected for composite restoration fillings. All restorations were performed by the same dentist, following an identical clinical protocol, including the same finishing and polishing procedures for all restorations. All 20 patients were instructed to follow the same oral hygiene protocol, which included standardized tooth brushing techniques and the use of mouth rinses. After four months, all patients were recalled for follow-up and data collection (Hamad & Atiyea, 2021).

2.3.2. Antibacterial Activity

Antibacterial activity of the nanocomposite was determined by using a well-diffusion method for *S. mutans, S. mitis,* and *S. lentus*. The culture was inoculated by the spread plate method. Nutrient agar was used to subculture bacteria and was incubated at 37℃ for 24 h. Mueller-Hinton agar plates were inoculated with pathogenic bacteria. Sterile well- diffusion of 5 mm diameter, saturated with plant extract as a control and nanocomposite were placed in each plate. The plates were then incubated for 24 h at 37°C. The inhibition zones were measured and recorded (Lavaee et al., 2022). All antibacterial experiments were performed in quadruplicate ($n = 4$) to ensure reproducibility and reliability of the results. The inhibition zone diameters were measured independently for each replicate, and the results were expressed as mean ± standard deviation.

2.3.3. Cytotoxicity

The cytotoxicity of the biosynthesized Cobalt-Copper-Chromium nanocomposite was evaluated using the MTT assay on normal HDF cells. Cells were seeded in 96-well plates and allowed to adhere for 24 h. Subsequently, the cells were exposed to different dilutions of the nanocomposite for 48 h under standard culture conditions (37°C, 5% CO_2). After incubation, MTT solution was added, and the formation of formazan crystals was measured spectrophotometrically.

2.4. Statistical Analysis

All experiments were performed in quadruplicate ($n = 4$), and the results were expressed as mean ± standard deviation (SD). Statistical analysis was conducted using one-way analysis of variance (ANOVA) to evaluate the significant differences between the tested concentrations of the nanocomposite against the bacterial strains. When significant differences were detected, Tukey's post-hoc test was applied for multiple comparisons. A p-value < 0.05 was considered statistically significant. Statistical analysis was carried out using GraphPad Prism (version 9.0) software.

3. RESULTS AND DISCUSSION

3.1. FT-IR Characterization of $Co_3CuCr_2O_8$ Nanocomposite

The FT-IR analysis was utilized to identify the different functional groups present in *O. europaea leaf* extract, which can be responsible for the reduction of cobalt, copper, and chromium salts to $Co_3CuCr_2O_8$ Nanocomposite and play roles as efficient capping and stabilization agents (Pasieczna-Patkowska et al., 2025). Figure 1(A) shows a typical FT-IR spectrum for *O. europaea leaf* extract along with a comparison with Figure 1(B), which shows $Co_3CuCr_2O_8$ Nanocomposite synthesized using this extract.

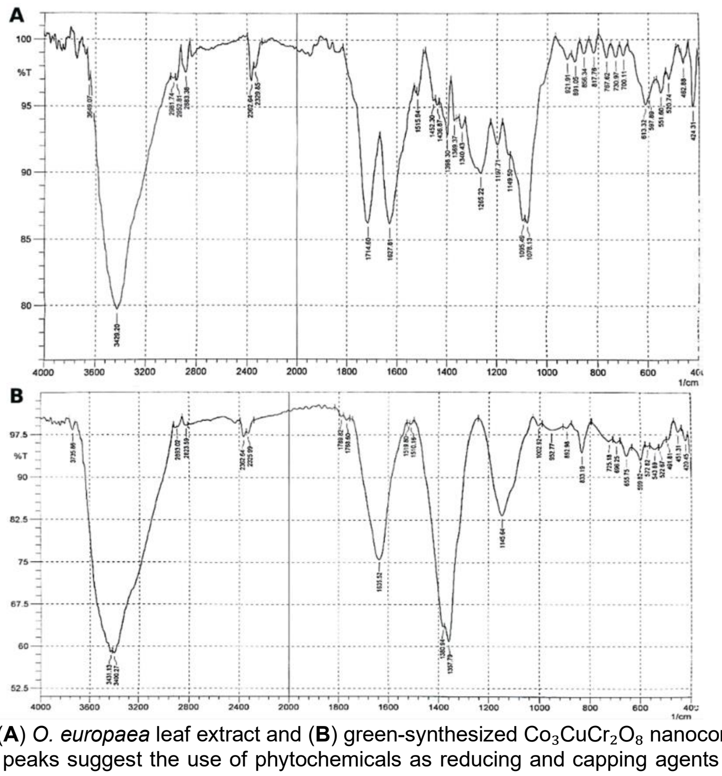

Figure 1. FTIR Spectra of (**A**) *O. europaea* leaf extract and (**B**) green-synthesized $Co_3CuCr_2O_8$ nanocomposite. The changes in the spectrum and shifts in peaks suggest the use of phytochemicals as reducing and capping agents in the production of the nanocomposite.

Comparison of these two spectra indicated that a new peak appears at 3735 cm^{-1} likely indicating the presence of a free OH group (not involved in hydrogen bonding). Previously, the carbonyl group (C=O) shifted or changed at 1714 cm^{-1}, this peak is altered in the second spectrum (new peaks around 1768 and 1789 cm^{-1}). Additional peaks appear between 1500-1000 cm^{-1} such as 1519, 1510, 1380, 1357, 1145, and 1002 cm^{-1}. These regions are rich in functional group vibrations, like C-O or C-N. Peak at 3400 cm^{-1}. Comparable to the earlier peak (3429 cm^{-1}) and suggests continued presence of OH or NH groups involved in hydrogen bonding, indicating the binding of cobalt, copper, and chromium ions with the hydroxyl, carbonyl, and amide groups of the leaf extract. The results also indicate that the phytochemicals in *O. europaea* leaf extract act as reducing and stabilizing (capping) agents in the synthesis of nanoparticles. Polyphenols, flavonoids and phenolic acids have a high number of hydroxyl and carbonyl groups, which can chelate metal ions and donate electrons, which is useful for the reduction of metal ions into stable metal oxide nanostructures. The observed changes in the FTIR absorption bands, therefore, provide strong evidence of interaction between biomolecules from plants and the surface of nanoparticles, which leads to an increase in the stability of nanoparticles and a decrease in aggregation.

3.2. Structural, Morphological, and Optical Properties of Synthesized Nanostructures

The structure of the samples was investigated by X-ray diffraction. All the scans have been recorded by SHIMADZU XRD-6000, with Cu Kα radiation line of λ=1.54˚A in the 2θ range from 10◦ to 80◦. The patterns of the nanocomposite (Issa et al., 2022; Hasanin et al., 2024). The XRD pattern shows a significant broadening of lines, which are characteristic of nanosized particles. The crystallite size can be calculated according to the Debye-Scherrer equation(Fatimah et al., 2022). Figure (2) shows the XRD pattern of Cobalt-Copper-Chromium nanocomposite Nine Characteristic peaks are observed at 2θ=20.8°, 25.4°, 26.5°,29.2°, 31.1°, 36.8°,44.9°and 54.1°in the XRD pattern, which corresponds to the (100), (111), (200), (211), (220), (311), (400) and (422) crystal planes of nanocomposites (Selvanayaki et al., 2022). From the results, it can be concluded that broader peaks refer to smaller particle sizes, which reflect good conditions for crystal growth. The Scherrer formula was used to determine the average crystal size of the nanocomposite, and the result was approximately 16.3 nm. The relatively small crystallite size is beneficial for biomedical applications because the nanoscale crystallites have a higher surface-to-volume ratio, which means that there are more surface atoms that can interact with the bacterial cells. Furthermore, smaller crystallites are likely to lead to higher ion release and generation of Reactive Oxygen Species (ROS) which are important for the antimicrobial activity of metal oxide nanocomposites.

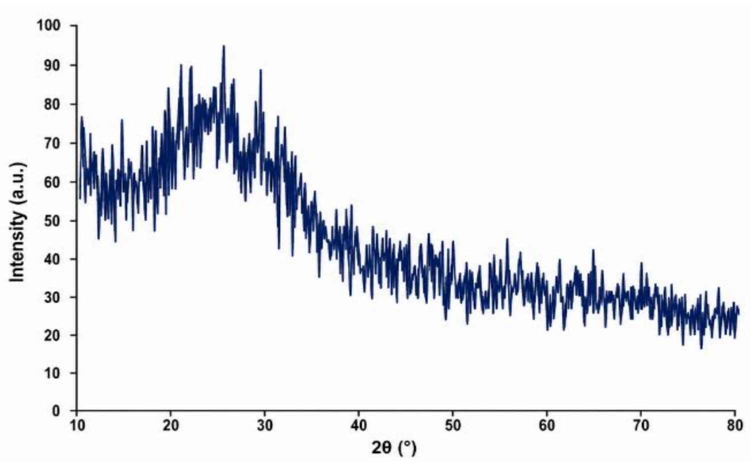

Figure 2. X-ray diffraction (XRD) pattern of green-synthesized $Co_3CuCr_2O_8$ nanocomposite using Olea europaea leaf extract. The diffraction peaks show that the synthesized nanocomposite is crystalline.

FESEM was used to investigate the morphology and size distribution of different nanocomposites, as shown in Figure 3. FESEM shows surface morphology and particle aggregation. The samples contain high porosity through the measurement images. Porous morphology may increase the surface area of nanoparticles. The spherical shape is the dominant one in the samples (Liu et al., 2022). The nanoparticle size ranged between 45.75 and 51.67 nm. Some clusters are present in the samples in very low percentages; however, this occurred during sample preparation by the examiner when preparing the sample for measurement. The produced spherical aggregates with a nearly uniform distribution in the samples can be concluded from FESEM analysis. In addition, the crystal nature of equal-sized synthesized nanocomposites is demonstrated. There are high proportions of homogeneous diameters in measurement images and small sizes. These results are nearly identical to those obtained from the XRD pattern. The slight aggregation seen in FESEM images is a common phenomenon for biosynthesized metal oxide nanoparticles and is primarily due to the magnetic interaction between the nanoparticles and their high surface energy. However, the aggregation was not extensive, indicating that the phytochemicals of *O. europaea* were able to stabilize the nanoparticles and inhibit excessive growth.

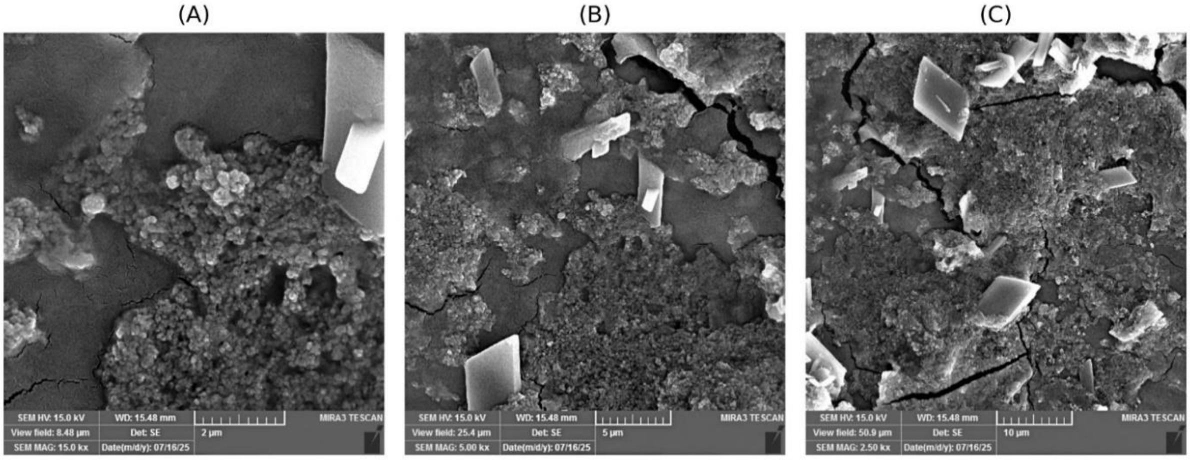

Figure 3. Images of the green-synthesized $Co_3CuCr_2O_8$ nanocomposite obtained using FESEM. (**A**) 15.0 k× magnification (2 μm scale bar), (**B**) 5.0 k× magnification (5 μm scale bar), and (**C**) 2.5 k× magnification (10 μm scale bar).

The EDX spectrum of the cobalt-copper-chromium nanocomposite synthesized is shown in Figure (4). Typical Co,Cr,Cu and oxygen peaks are present in the spectrum. The results confirm the presence of Co, Cu, Cr and O elements of the synthesized nanostructures (Moro et al., 2021; Sudha et al., 2023). The EDX spectrum also does not show other peaks of impurities, which further confirms the high purity of the synthesized nanocomposite. This indicates that the green synthesis method was able to produce the desired ternary metal oxide without significant contamination from the precursor salts or other impurities. Furthermore, the EDX measurement was equal for: cobalt 52.3, chromium 27.8, copper 20.3 and oxygen 11.5. There are many types of X-ray maps, which include dot mapping, regions of interest (ROI) mapping, background-subtracted and overlap-corrected mapping, quantitative mapping, and full spectrum mapping (or spectrum mapping). The mapping of the Cobalt-Copper-Chromium nanocomposite synthesized is shown in Figure 4.

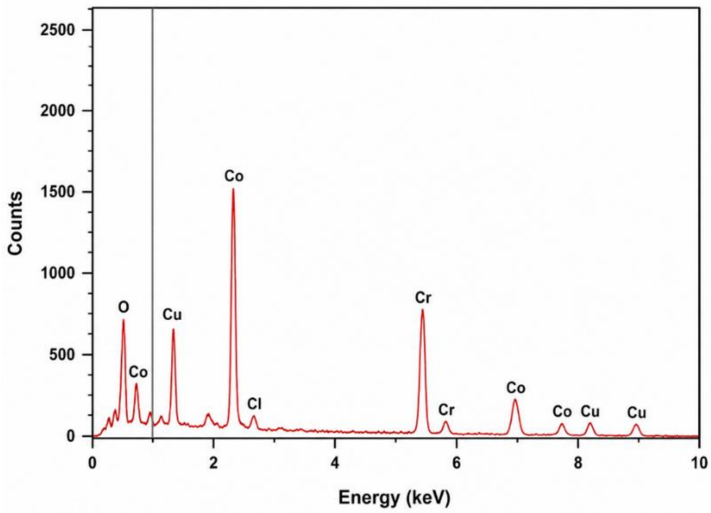

Figure 4. Energy-dispersive X-ray spectroscopy (EDX) spectrum of the green-synthesized $Co_3CuCr_2O_8$ nanocomposite. The successful formation of the ternary metal oxide nanocomposite is confirmed by the elemental analysis.

TEM micrographs in Figure 5 revealed predominantly spherical nanoparticles. Image analysis yielded a mean particle size of ~51.3 nm. The TEM micrograph reveals the formation of dark-contrast nanoscale particles, confirming the successful synthesis of metal oxide nanoparticles. The high electron density of the particles is attributed to the presence of transition metals (Co, Cu, and Cr), which strongly scatter the electron beam. Figure 5A shows that the particles appear irregular to quasi-spherical in morphology, which is typical for nanoparticles synthesized via green reduction routes. In plant-mediated synthesis, phytochemicals such as polyphenols, flavonoids, tannins, and terpenoids present in *O. europaea* leaf extract act as both reducing and capping agents.

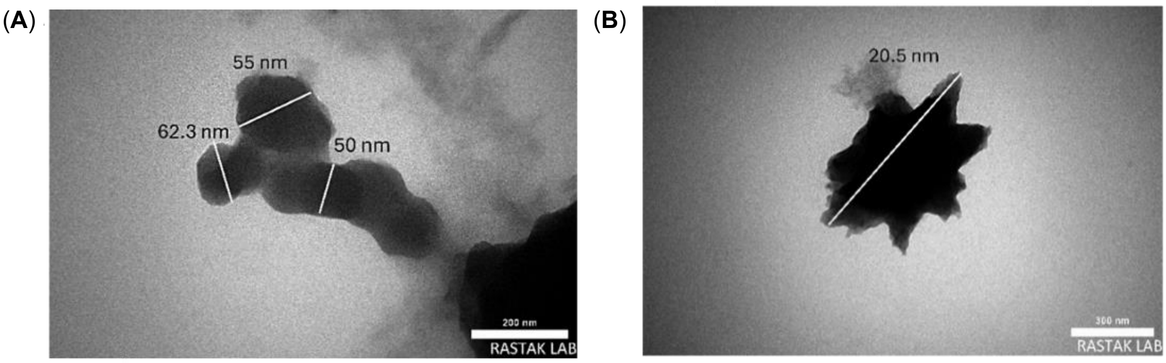

Figure 5. TEM images of green-synthesized $Co_3CuCr_2O_8$ nanocomposite. (**A**) The aggregated quasi-spherical nanoparticles are between about 50 and 62.3 nm in particle size. (**B**) Single nanoparticle, particle size ~ 20.5 nm, nanoscale morphology and particle aggregation.

Polyphenolic compounds (e.g.,ellagic acid,gallic acid,caffeic acid, ferulic acid, *p*-coumaric acid, and quercetin). Inactivate the metal ions by chelation via their adjacent phenolic hydroxyl groups and are oxidized to the corresponding quinones. The metal ions are reduced to zero-valent nanoparticles by the transfer of free electrons and protons during the bioreduction, indicating that the green synthesis approach successfully produced metal oxide nanoparticles. The non-uniform surface features and mild edge roughness indicate that the nanostructures are likely made up of several crystallites aggregated together, a typical characteristic of biosynthesized metal oxide nanoparticles leading to anisotropic growth and slightly irregular particle shapes. The observed particle size is approximately 20.5 nm. Figure 5B shows a TEM micrograph with aggregated nanostructures forming chain-like clusters, with particle sizes measured at approximately 50 nm, 55 nm, and 62.3 nm. These larger dimensions likely represent nanoparticle aggregates rather than single primary particles.

Agglomeration is frequently observed in multimetal oxide nanocomposites, particularly those synthesized using plant extracts. This phenomenon can be attributed to the magnetic interaction of cobalt oxide components, which can induce particle attraction; the high surface energy of nanoscale metal oxides, encouraging particles to cluster in order to minimize total surface energy; and Organic residues from *O. europaea* leaf extract phytochemicals, which may partially coat the nanoparticle surface and promote controlled aggregation. The formation of clustered nanostructures suggests strong interaction among the Co, Cu, and Cr oxide phases, leading to the formation of a heterogeneous nanocomposite structure rather than isolated nanoparticles. These phytochemicals adsorb on the nanoparticle surface, limiting uncontrolled growth and producing nanostructures in the 20–60 nm range, as observed in the TEM images. The size of the particles seen in TEM was slightly larger than the crystallite size determined by XRD, suggesting that each nanoparticle is a collection of several crystallites. This is often seen as a difference since XRD measures the crystallite size while TEM measures the physical size of the whole nanoparticles.

3.3. Antimicrobial Assay of Cobalt-Copper-Chromium Nanocomposite

In the present study, the antibacterial effect of the nanoparticle was tested against *S. mutans, S. mitis,* and *S. lentus* (Jaafar & Hammood, 2024; Sami et al., 2025). The nanomaterial tested in this study exhibited varying levels of antibacterial activity against the three isolated bacterial species, depending on the concentration used. Figure 6 and Table 1 showed the results on *S. mitis, which* showed clear sensitivity to the nanomaterial at concentrations of 50 µg/mL and above. At 100 µg/mL, a 20 mm inhibition zone was observed, indicating strong antibacterial activity. At both 75 µg/mL and 50 µg/mL, the inhibition zone was 15 mm, showing moderate effectiveness. No inhibition was observed at 25 µg/mL, suggesting this concentration is insufficient to affect the growth of *S. mitis*. These findings demonstrate that the nanomaterial begins to be effective at 50 µg/mL, with increased potency at higher concentrations. As for *S. mutans*. A similar pattern was observed for *S. mutans*, although the sensitivity was slightly lower at intermediate concentrations. At 100 µg/mL, the inhibition zone was 19 mm, reflecting a strong antibacterial effect. At 75 µg/mL, a 15 mm zone was seen, and at 50 µg/mL, a 12 mm zone was measured, both showing moderate inhibition. No inhibition was recorded at 25 µg/mL, indicating low activity at this level. The gradual increase in the inhibition zone confirms that the material's effectiveness increases with concentration (Mendes et al., 2022).

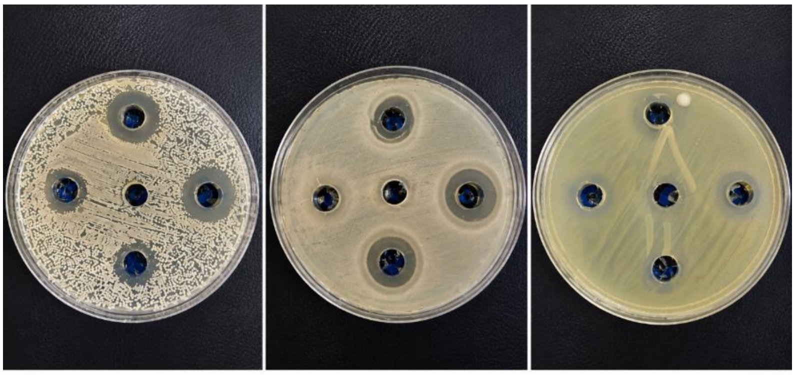

Figure 6. Antibacterial activity of green-synthesized $Co_3CuCr_2O_8$ nanocomposite against oral pathogenic bacteria (*S. mutans*, *S. mitis* and *S. lentus*) was carried out by agar well diffusion assay.

Regarding *S. lentus*, it showed more resistance to the nanomaterial compared to the *Streptococcus* species. At 100 µg/mL, a 20 mm inhibition zone was observed, indicating good sensitivity at maximum concentration. At 75 µg/mL, a 15 mm zone was observed, but no inhibition was seen at 50 µg/mL or 25 µg/mL. These results suggest that *S. lentus* requires a higher concentration of the nanomaterial to achieve bacterial inhibition, possibly due to differences in cell wall structure or resistance mechanisms. Statistical analysis using one-way ANOVA demonstrated significant differences in the antibacterial activity of the synthesized Co-Cu-Cr nanocomposite at different concentrations ($p < 0.05$). The inhibition zones increased significantly with increasing nanocomposite concentration, confirming a dose-dependent antibacterial effect. *S. mitis* and *S. mutans* showed significantly higher sensitivity compared to *S. lentus*, which required higher concentrations to achieve bacterial inhibition. The statistical significance indicates that the antibacterial activity observed is reliable and not due to experimental variation.

Table 1. Antibacterial activity against oral bacterial isolates as inhibition zone diameter (mm, mean ± SD; n = 4).

Bacterial strain	Concentration	Inhibition zone (mm) Mean ± SD	Significance (p-value)
S. mitis	25 µg/mL	0 ± 0	–
	50 µg/mL	15 ± 0.8	p < 0.05
	75 µg/mL	15 ± 0.7	p < 0.05
	100 µg/mL	20 ± 1.0	p < 0.01
S. mutans	25 µg/mL	0 ± 0	–
	50 µg/mL	12 ± 0.9	p < 0.05
	75 µg/mL	15 ± 0.6	p < 0.05
	100 µg/mL	19 ± 0.8	p < 0.01
S. lentus	25 µg/mL	0 ± 0	–
	50 µg/mL	0 ± 0	–
	75 µg/mL	15 ± 0.7	p < 0.05
	100 µg/mL	20 ± 1.1	p < 0.01

First, the nanoparticles may bind to the bacterial cell wall via electrostatic interaction, which would lead to the alteration of the integrity of the cell wall and make the cell wall more permeable. Second, the nanocomposite could produce reactive oxygen species (ROS), such as hydroxyl radicals and superoxide ions, that cause oxidative stress, causing lipid peroxidation, protein denaturation, and DNA damage. Moreover, the slow release of Co^{2+}, Cu^{2+} and Cr^{3+} ions could disrupt the key metabolic pathways and enzyme activities of the bacteria, leading to their death. These mechanisms give the ternary nanocomposite superior performance to nanoparticles of a single metal oxide.

3.4. Cytotoxicity

MTT data showed a dose-dependent reduction in viability after 48 h, as shown in Figure 7. The dose-dependent decrease in cell viability suggests that the toxicity of the nanocomposite is highly dependent on the amount of nanoparticles. This concentration-dependent cytotoxicity is similar to previous studies of metal oxide nanoparticles, which found that higher concentrations of nanoparticles led to greater cellular uptake, oxidative stress, and mitochondrial dysfunction. Too many ROS can cause cellular damage to proteins, lipids and DNA, which will eventually affect cell viability.

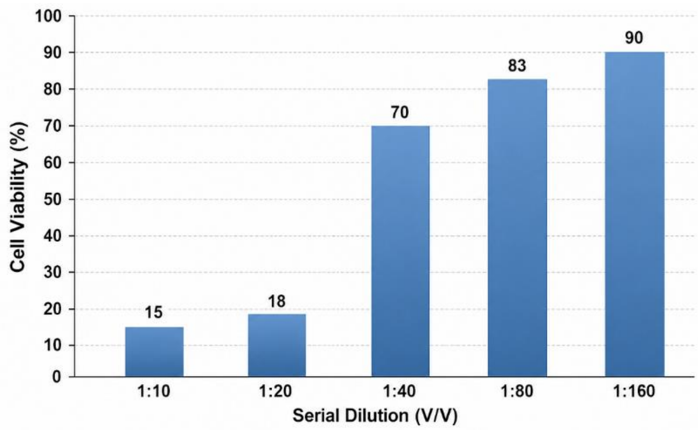

Figure 7. The green-synthesized $Co_3CuCr_2O_8$ nanocomposite was found to be cytotoxic to normal HDF cells after 48 h exposure by MTT assay.

Importantly, cell viability was maintained above 80% at higher dilutions, indicating cytocompatibility at controlled exposure concentrations. The results indicate that the cell viability increased with dilutions, which indicates that cells were less stressed with lower concentrations of nanoparticles, while still maintaining good biocompatibility. This discovery underscores the need for careful optimization of the dose of nanoparticles to ensure a balance between antimicrobial efficacy and safety of the host cells for biomedical applications. To achieve this balance between antibacterial activity and low cytotoxicity, nanocomposite-based dental materials that will be in contact with oral tissues for a long time should be developed in the future. In the clinical aspect, the use of $Co_3CuCr_2O_8$ nanocomposites in restorative dental materials, adhesives or protective coatings can help to minimize bacterial colonization, biofilm formation and hence secondary caries. Multifunctional nanocomposites could help in the durability of dental restorations and reduce the necessity for frequent restorative treatments. The current results show excellent cytocompatibility, but additional tests with oral cell lines, long-term tests, and in vivo tests are required to ensure the safety and clinical potential of the synthesized $Co_3CuCr_2O_8$ nanocomposite in dental applications.

4. CONCLUSION

A nanocomposite was successfully prepared by green synthesis, and the method is considered cheap, safe, easy to use, and fast to produce. The nanocomposites were characterized by several techniques, the most important of which are FTIR, XRD, FESEM, and EDX. Comparison of these two spectra indicated that a new peak appears at 3735 cm^{-1}, likely indicating the presence of a free OH group (not involved in hydrogen bonding). The carbonyl group (C=O) shift or change was previously at 1714 cm^{-1}. This peak is altered in the second spectrum (new peaks around 1768 and 1789 cm^{-1}). New peaks between 1500-1000 cm^{-1} include:1519, 1510, 1380, 1357, 1145, 1002. These regions are rich in functional group vibrations, like C-O or C-N. Peak at 3400 cm^{-1}. Comparable to the earlier peak (3429 cm^{-1}) and suggests continued presence of OH or NH groups involved in hydrogen bonding, indicating the binding of cobalt, copper, and chromium ions with the hydroxyl, carbonyl, and amide groups of the leaf extract. The crystallite size of the nanocomposite was 16.3 nm; the size of nanoparticles was 45.7-51.6 nm. The difference between this number is the larger particle size compared to the crystallite size indicates that the nanoparticles are composed of several crystallites, forming polycrystalline aggregates rather than single crystals. The antibacterial effect of the nanomaterial in this study demonstrated a clear dose-dependent response against all three bacterial isolates (*S. mitis*, *S. mutans*, and *S. lentus*). As the concentration increased, the antibacterial action, its ability to inhibit bacterial growth, also increased. The size of the inhibition zones, a common measure of antibacterial effectiveness, grew larger with higher concentrations, indicating stronger antibacterial activity. This dose-dependency is a desirable property for antimicrobial agents, as it suggests that the material's effectiveness can be modulated and optimized based on the required clinical application.

S. mitis and *S. mutans*, which are two of the most prominent bacterial species involved in the initiation and progression of dental plaque and secondary caries, were both inhibited starting at a 50µg/mL concentration of the nanomaterial. At the highest concentration tested (100µg/mL), the inhibition zones reached 20 mm and 19 mm, respectively. These results are significant because they show that the nanomaterial is particularly effective against Gram-positive oral streptococci, which are known to be among the first colonizers of tooth surfaces. Their early adhesion paves the way for the development of complex biofilms, which are more resistant to conventional treatments. Therefore, inhibiting these bacteria at early stages is crucial in preventive dental strategies.

In contrast, *S. lentus*, although also Gram-positive, exhibited more resistance to the nanomaterial. It displayed no inhibition at concentrations of 50 µg/mL or below, and only began to display susceptibility at higher concentrations (75 µg/mL and 100 µg/mL), with inhibition zones of 15 mm and 20 mm, respectively. This suggests that *S. lentus* may have more robust defense mechanisms or structural characteristics that render it less sensitive to the nanomaterial at lower doses. Possible factors include a thicker or differently composed cell wall, variations in surface proteins, or more efficient stress response systems that help it survive in hostile environments. These differences highlight the importance of tailoring antimicrobial approaches to target specific bacterial characteristics.

Taken together, the findings indicate that the nanomaterial possesses broad-spectrum antibacterial activity, but its full potential is most evident at concentrations of 75µg/mL and above. This dose threshold is critical when considering clinical applications. This study has some limitations, however, in spite of the promising findings. The synthesized $Co_3CuCr_2O_8$ nanocomposite was only tested for antibacterial activity by the agar well diffusion assay, necessitating further testing such as minimum inhibitory concentration, minimum bactericidal concentration, and antibiofilm assays to fully evaluate its antimicrobial activity. Secondly, the cytotoxicity test was conducted only in human dermal fibroblast cells after 48 h of exposure and is recommended to be extended to oral cell lines including human gingival fibroblasts or dental pulp stem cells and long-term biocompatibility studies. Lastly, the antibacterial activity of the nanocomposite against selected oral pathogens was found to be promising, but it was not evaluated in dental restorative materials, and its effect on mechanical, physicochemical, and long-term stability properties of such materials was not studied. These factors should be taken into consideration in future studies, and in vivo evaluation should be performed to validate the clinical use of the nanocomposite synthesized.

ACKNOWLEDGEMENT
The authors sincerely thank all individuals who contributed to the successful completion of this study.

CONFLICT OF INTEREST
The authors declare no conflicts of interest.

AUTHOR CONTRIBUTION
Riyam Lateef Khalaf: Conceptualization, methodology, and software. Mina Mohammed Kadhim: Data collection and writing original draft. Abdalwahab Malath Alhadithi: Visualization and investigation. Ola Abdul Kareem Nori: Supervision, software, validation, writing, review, and editing.

DATA AVAILABILITY
All data generated or analyzed during this study are included in this published article.

DECLARATION OF GENERATIVE AI
Not applicable.

ETHICS
Not applicable.

REFERENCES

Ahmadian E, Shahi S, Yazdani J, Dizaj SM, Sharifi S. (2018). Local treatment of the dental caries using nanomaterials. *Biomedicine & Pharmacotherapy*, 108, 443-447. doi:10.1016/j.biopha.2018.09.026

Al-Deen AHA, Mahmood RI, Ali SM, Mohammed-Salih HS, Jamaludin AA, Al-Obaidi JR. (2026). Green-synthesized tricalcium silicate nanoparticles from *Salvia officinalis* for antimicrobial coating of clear aligners and prevention of enamel demineralization. *Next Nanotechnology*, 9, 100427. doi:10.1016/j.nxnano.2026.100427

Engen SA, Rørvik GH, Schreurs O, Blix IJ, Schenck K. (2017). The oral commensal *Streptococcus mitis* activates the aryl hydrocarbon receptor in human oral epithelial cells. *International Journal of Oral Science*, 9, 145-150. doi:10.1038/ijos.2017.17

Esfanddarani HM, Panigrahi M. (2024). Phytosynthesis of transition (Ni, Fe, Co, Cr, and Mn) metals and their oxide nanoparticles for biomedical applications: a review. *Journal of Materials Science*, 59, 10677-723. doi:10.1007/s10853-024-09800-4

Fatimah S, Ragadhita R, Al Husaeni DF, Nandiyanto ABD. (2022). How to calculate crystallite size from x-ray diffraction (XRD) using Scherrer method. *ASEAN Journal of Science and Engineering*, 2, 65-76. doi:10.17509/ajse.v2i1.37647

Hamad AM, Atiyea QM. (2021). In vitro study of the effect of zinc oxide nanoparticles on *Streptococcus mutans* isolated from human dental caries. *Proceedings of the Journal of Physics: Conference Series*, 1879, 022041. doi:10.1088/1742-6596/1879/2/022041

Hasanin MS, Saeb MR, Abdel-Maksou MA, El-Tayeb MA, Kiani BH, Hashem AH. (2024). Advanced functional Cu-Cr-Co-NPs@ gelatin (GLN)-hydroxyethyl cellulose (HEC) nanocomposites with antimicrobial and anticancer activities. *RSC Advances*, 14, 37633-43. doi:10.1039/d4ra06216g

Issa HK, Maleki A, Taherizadeh A, Zargaran A. (2022). On the structure-properties relationship of amorphous and crystalline silica nanoparticles reinforced magnesium matrix nanocomposites. *Journal of Alloys and Compounds*, 924, 166605. doi:10.1016/j.jallcom.2022.166605

Jaafar RS, Hammood AY. (2024). Antibacterial activity and cytotoxicity of spinel copper ferrite nanoparticles synthesized by using sol gel technique and lemon juice as substrate. *Pollution*, 10, 63-72. doi:10.22059/poll.2023.361453.1967

Jaffar S, Taj MK, Taj I, Khan MA, Azam S, Khan S, Essote S, Samreen Z, Jaffar H. (2023). Factors responsible for dental caries among patients and its management. *Pak-Euro Journal of Medical and Life Science*, 4(1), 196-209. doi:10.31580/pjmls.v4iS

Jeon TH, Wu Z-Y, Chen F-Y, Choi W, Alvarez PJ, Wang H. (2022). Cobalt–copper nanoparticles on three-dimensional substrate for efficient ammonia synthesis via electrocatalytic nitrate reduction. *The Journal of Physical Chemistry C*, 126, 6982-6989. doi:10.1021/acs.jpcc.1c10781

Joy A, Unnikrishnan G, Megha M, Haris M, Thomas J, Kolanthai E, Muthuswamy S. (2022). Polycaprolactone/graphene oxide-silver nanocomposite: a multifunctional agent for biomedical applications. *Journal of Inorganic and Organometallic Polymers and Materials*, 32, 912-930. doi:10.1007/s10904-021-02180-1

Khalaf RL, Ahmed EM. (2019). Biosynthesis of silver nanoparticles using plants flowers of *Nerium oleander* extract and its antibacterial activity. *Biochemical & Cellular Archives*, 19, 263.

Khalaf RL, Ahmed EM, Mathkor TH, Al-Zubaidi HY. (2021a). Synthesis of silver nanoparticles using L. rosa flowers extracts: Thermodynamic and kinetic studies on the inhibitoty effects of nanoparticles on creatine kinase activity. *Iraqi Journal of Science*, 62(8), 2486-2500. doi:10.24996/ijs.2021.62.8.1

Khalaf RL, Almousawi IM, Rheima AM. (2021b). Dye pollution removal in aqueous solution using novel photochemically synthesized $CoZnFe_2O_5$ nanocomposite. *Desalination and Water Treatment*, 243, 287-93. doi:10.5004/dwt.2021.27892

Khudiar SS, Nayef UM, Mutlak Fa-H, Abdulridha SK. (2022). Characterization of NO_2 gas sensing for ZnO nanostructure grown hydrothermally on porous silicon. *Optik*, 249, 168300. doi:10.1016/j.ijleo.2021.168300

Lavaee F, Motamedifar M, Rafiee G. (2022). The effect of photodynamic therapy by gold nanoparticles on Streptococcus mutans and biofilm formation: An in vitro study. *Lasers in Medical Science*, 37, 1717-25. doi:10.1007/s10103-021-03422-x

Lemos JA, Palmer SR, Zeng L, Wen ZT, Kajfasz JK, Freires IA, Abranches J, Brady LJ. (2019). The Biology of *Streptococcus mutans*. *Microbiology Spectrum*, 7, 1-18. doi:10.1128/microbiolspec.gpp3-0051-2018

Liu A, Liu S, Liu Y, Liu B, Liu T. (2022). Characterizing mechanical heterogeneity of coal at nano-to-micro scale using combined nanoindentation and FESEM-EDS. *International Journal of Coal Geology*, 261, 104081. doi:10.1016/j.coal.2022.104081

Mamidi N, Delgadillo RM, Sustaita AO, Lozano K, Yallapu MM. (2025). Current nanocomposite advances for biomedical and environmental application diversity. *Medicinal Research Reviews*, 45, 576-628. doi:10.1002/med.22082

Mendes CR, Dilarri G, Forsan CF, Sapata VMR, Lopes PRM, de Moraes PB, Montagnolli RN, Ferreira H, Bidoia ED. (2022). Antibacterial action and target mechanisms of zinc oxide nanoparticles against bacterial pathogens. *Scientific Reports*, 12, 2658. doi:10.1038/s41598-022-06657-y

Mohammed-Salih HS, Ghazi A, Mahmood RI, Al-Qazzaz HH, Supian FL, Al-Obaidi JR, Jabir M. (2024). Enhancing orthodontic treatment control with fish scale-derived hydroxyapatite nanoparticles: Insights from an animal model study. *The Saudi Dental Journal* 36, 1128-34. doi:10.1016/j.sdentj.2024.06.007

Mohammed-Salih HS, Mahmood RI, Ghazi A, AlQrimli AF, Rashid TM, Al-Obaidi JR, Supian FL, Jabir MS. (2025). Antibacterial effect of novel orthodontic PEEK beads coated with a conjugate of fish scale hydroxy-apatite nanoparticles and GL13K peptide. *BioNanoScience*, 15, 557. doi:10.1007/s12668-025-02188-8

Moro D, Ulian G, Valdre G. (2021). SEM-EDS nanoanalysis of mineral composite materials: A Monte Carlo approach. *Composite Structures*, 259, 113227. doi:10.1016/j.compstruct.2020.113227

Pasieczna-Patkowska S, Cichy M, Flieger J. (2025). Application of Fourier transform infrared (FTIR) spectroscopy in characterization of green synthesized nanoparticles. *Molecules*, 30(3), 684. doi:10.3390/molecules30030684

Sami RH, Jawad SF, Zankanah FH, Jawad KH, Hasoon BA, Issa AA, Jabir MS, Al-azawi KF. (2025). Biosynthesis of platinum nanoparticles: Evaluation of their activity against streptococcus mutans and in silico study. *Plasmonics*, 20, 3413-3427. doi:10.1007/s11468-024-02543-7

Saratale RG, Saratale GD, Shin HS, Jacob JM, Pugazhendhi A, Bhaisare M, Kumar G. (2018). New insights on the green synthesis of metallic nanoparticles using plant and waste biomaterials: current knowledge, their agricultural and environmental applications. *Environmental Science and Pollution Research*, 25, 10164-10183. doi:10.1007/s11356-017-9912-6

Selvanayaki R, Rameshbabu M, Muthupandi S, Razia M, Sasi Florence S, Ravichandran K, Prabha K. (2022.) Structural, optical and electrical conductivity studies of pure and Fe doped Zinc oxide (ZnO) nanoparticles. *Materials Today: Proceedings*, 49, 2628-2631. doi:10.1016/j.matpr.2021.08.045

Shafey AE. (2020). Green synthesis of metal and metal oxide nanoparticles from plant leaf extracts and their applications: a review. *Green Processing and Synthesis*, 9(1), 304-339. doi:10.1515/gps-2020-0031

Shao Q, Feng D, Yu Z, Chen D, Ji Y, Ye Q, Cheng D. (2023). The role of microbial interactions in dental caries: Dental plaque microbiota analysis. *Microbial Pathogenesis*, 185, 106390. doi:10.1016/j.micpath.2023.106390

Sudha D, Kumar ER, Shanjitha S, Munshi AM, Al-Hazmi GAA, El-Metwaly NEM, Kirubavathy SJ. (2023). Structural, optical, morphological and electrochemical properties of ZnO and graphene oxide blended ZnO nanocomposites. *Ceramics International*, 49, 7284-7288. doi:10.1016/j.ceramint.2022.10.192

Tariq T, Ali A, Alvi F. (2026). Fabrication and characterization of Co_3O_4–Fe_2O_3–chitosan based ternary nanobiocomposite electrode for norepinephrine detection. *Sensor Review*, 1-10. doi:10.1108/SR-06-2025-0450

Umai D, Vikranth A, Meenambiga SS. (2021). A study on the green synthesis of silver nanoparticles from Olea europaea and its activity against oral pathogens. *Materials Today: Proceedings*, 44, 3647-3651. doi:10.1016/j.matpr.2020.10.681

Yadav K, Prakash S. (2017). Dental caries: A microbiological approach. *Journal of Clinical Infectious Diseases & Practice*, 2(1), 1-15. doi:10.4172/2476-213X.1000118

Yazdanian M, Rostamzadeh P, Rahbar M, Alam M, Abbasi K, Tahmasebi E, Tebyaniyan H, Ranjbar R, Seifalian A, Yazdanian A. (2022). The potential application of green-synthesized metal nanoparticles in dentistry: A comprehensive review. *Bioinorganic Chemistry and Applications*, 2311910. doi:10.1155/2022/2311910

Zhang JS, Chu CH, Yu OY. (2022). Oral microbiome and dental caries development. *Dentistry Journal*, 10, 184. doi:10.3390/dj10100184